Short Communication

Electrooxidation of Phenol on PtRh and PtRu Alloys in 0.1 M NaOH Solution

Boguslaw Pierozynski[*], *Tomasz Mikolajczyk, Grazyna Piotrowska*

Department of Chemistry, Faculty of Environmental Management and Agriculture, University of Warmia and Mazury in Olsztyn, Plac Lodzki 4, 10-957 Olsztyn, Poland
[*]E-mail: boguslaw.pierozynski@uwm.edu.pl

This communication reports on kinetics of phenol electrooxidation reaction (PhER), studied at PtRh and PtRu alloy electrodes in 0.1 M NaOH supporting solution. The kinetics of PhER were analysed based on potential-dependent, a.c. impedance-derived values of charge-transfer resistance and capacitance parameters. Finally, obtained results were compared to those recently recorded on polycrystalline Pt electrode surface under analogous experimental conditions.

1. INTRODUCTION

Phenolic compounds, due to their severe toxicity and low biodegradability belong to some of the most dangerous chemical contaminants of industrial wastewaters, concerning such important industry sectors, as: petro-chemistry, oil refineries and drug manufacturing plants [1-5]. In fact, modern electrochemical methods were found highly attractive for the oxidative destruction of phenolic compounds, especially as they usually offer non-complex infrastructure and environmentally-friendly systems [4, 6-9]. Electrooxidation of various phenolic chemicals has widely been investigated in scientific literature on a number of anodes, including: noble/semi-noble (e.g. Pt, Ir, Ru) and transitional metals (Ti, Sb, Sn, Pb), their oxides and mutual compositions for variable pH and temperature conditions [1, 6, 8, 9-11].

An initial stage of phenol oxidation is usually associated [6, 9, 12] with conversion of a phenol molecule to hydroquinone and benzoquinone species, which then become destructively oxidized to

produce carboxylic acids, and ultimately to form H_2O and CO_2 molecules (a simplified phenol electrochemical degradation pathway is shown in Fig. 1 below).
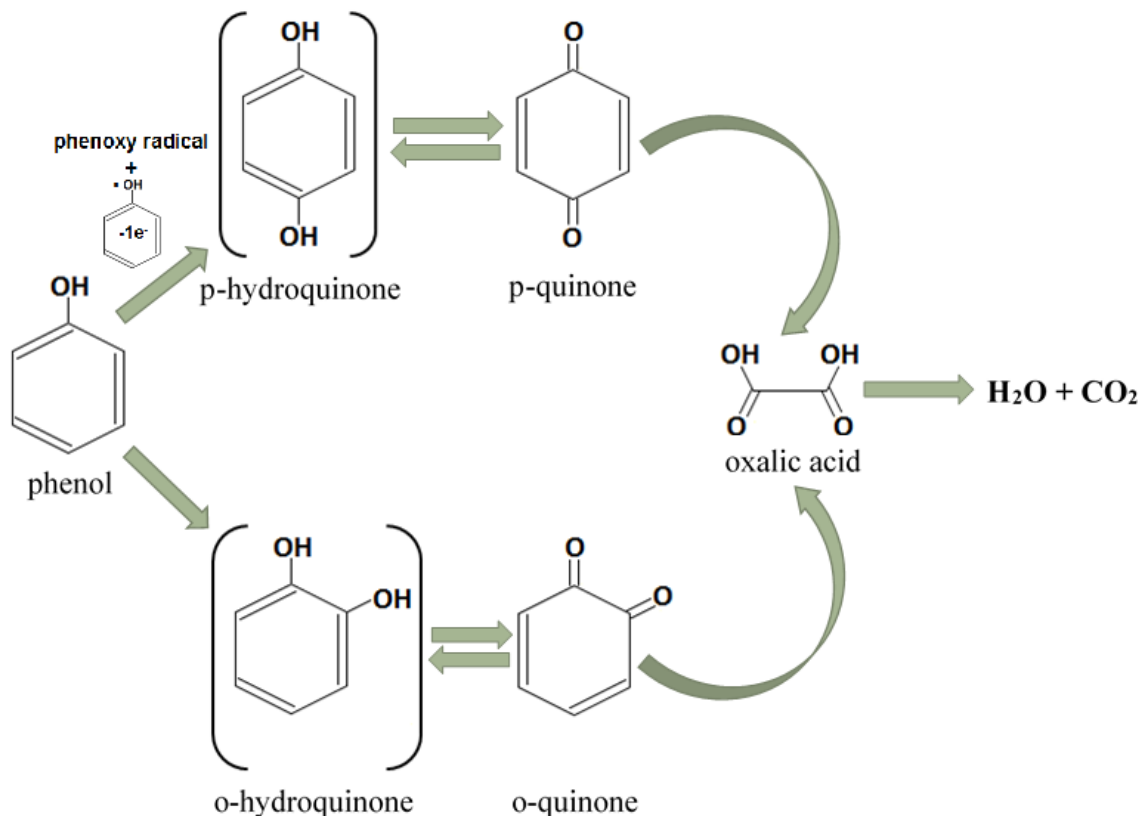
Figure 1. Schematic representation of electrochemical phenol degradation processes [1, 3-6, 9].

This communication is primarily concerned with the kinetic aspects of the phenol electrooxidation reaction, where the PhER is examined at PtRh and PtRu alloy electrode surfaces in 0.1 M NaOH supporting solution.

2. EXPERIMENTAL

Direct-Q3 UV ultra-pure water purification system from Millipore (18.2 MΩ cm water resistivity) was used to prepare 0.1 M NaOH solution from AESAR, 99.996 % NaOH pellets. Phenol concentration (Sigma-Aldrich, >99 %) was on the order of 1.2×10^{-2} M. An electrochemical cell, made of Pyrex glass, was used during the course of this work. The cell comprised three electrodes: a PtRh (Pt90/Rh10, 1 mm diameter alloy wire, Goodfellow) or PtRu (Pt95.2/Ru4.8, 0.05 mm thick alloy foil, AlfaAesar) working electrode (WE) in a central part, a reversible Pd (0.5 mm diameter wire of 99.9 % purity, Aldrich) hydrogen electrode (RHE) as reference and a Pt (1.0 mm diameter wire, 99.9998 % purity, Johnson Matthey, Inc.) counter electrode (CE), both placed in separate compartments (see details on the procedures for cleaning the cell and preparation of electrodes in Ref. 13).

Electrochemical a.c. impedance spectroscopy and cyclic voltammetry techniques were employed in this work. All measurements were performed at room temperature by means of the *Solartron* 12,608 W Full Electrochemical System, consisting of 1260 frequency response analyzer (FRA) and 1287 electrochemical interface (EI). The impedance experiments were carried-out at an a.c. signal of 5 mV and the frequency was swept between 1.0×10^5 and 0.5×10^{-1} Hz, whereas CV measurements were performed at a sweep-rate of 50 mV s^{-1}. The instruments were controlled by *ZPlot 2.9* (*Corrware 2.9*) software for Windows (Scribner Associates, Inc.), where data analysis was performed with *ZView 2.9* (*Corrview 2.9*) software package. The impedance spectra were fitted by means of a complex, non-linear, least-squares immitance fitting program, *LEVM 6*, written by J.R. Macdonald [14].

3. RESULTS AND DISCUSSION

The cyclic voltammetric behaviour of phenol (at 1.2×10^{-2} M) at PtRh and PtRu alloy electrode surfaces in 0.1 M NaOH is presented in Fig. 2 below.
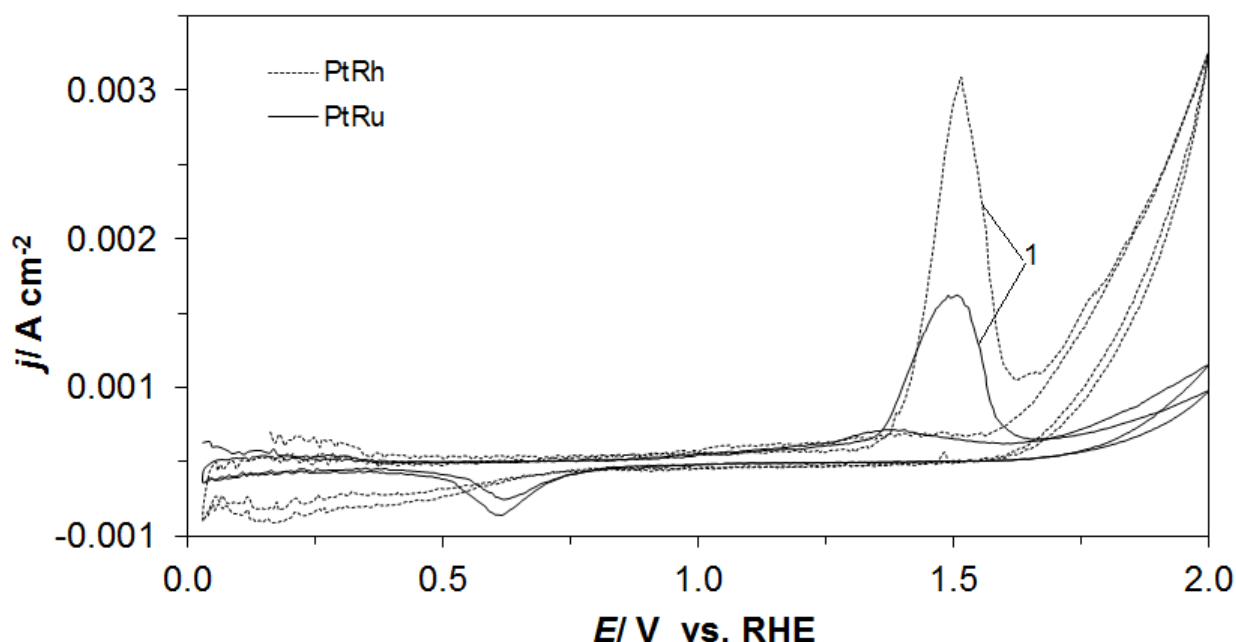
Figure 2. Cyclic voltammograms for electrooxidation of phenol (at 1.2×10^{-2} M) on PtRh and PtRu electrode surfaces, carried-out in 0.1 M NaOH supporting solution at a sweep-rate of 50 mV s^{-1} (1- indicates first voltammetric cycles).

Thus, a major anodic oxidation peak can be observed in the CV profiles over the potential range 1.3-1.6 V vs. RHE (radically increased current-density was recorded on the PtRh electrode alloy). This peak corresponds to an initial stage of phenol oxidation process (a single-electron charge-transfer step) producing a phenoxy radical cation (see Fig. 1), which could further be oxidized to

produce p/o-hydroquinone species, finally leading to oxidative destruction of the aromatic ring [1, 3, 4, 6, 9, 12]. Nevertheless, some of the phenoxy radicals that become adsorbed on the catalyst surface could couple to produce dimers and then polymeric compounds, leading to substantial blocking of the PtRh (PtRu) surface active sites, thus significantly inhibiting the PhER. The above could clearly be observed in the CV profiles of Fig. 2, where the high potential anodic peak becomes radically suppressed after several electrode cycles carried-out over the potential range 0.0-2.0 V. Furthermore, a broad cathodic reduction feature, observed for the PtRu electrode over the potential range *ca*. 0.5-0.8 V, could imply partial, but very limited reversibility of the phenol oxidation process on this electrode surface. Furthermore, voltammetric features observed on the PtRh electrode for the potentials just positive to the reversible potential are characteristic of significantly inhibited, reversible H UPD (hydrogen underpotential deposition) process at this electrode surface (Fig. 2). In addition, a considerable increase of anodic current-densities for the potentials positive to *ca*. 1.6 V (especially evident on the PtRh electrode) is associated with further surface oxidation processes (OH/O species electrosorption phenomena), prior to the Faradaic process of oxygen evolution reaction (OER).

Table 1. Resistance and capacitance parameters for the process of phenol electrooxidation (at 1.2×10^{-2} M) on PtRh and PtRu alloy electrode surfaces in contact with 0.1 M NaOH solution (at room temperature), obtained by fitting the equivalent circuit shown in Fig. 4 to the experimentally-obtained impedance data.

Electrooxidation of phenol at PtRh		
E/ mV	R_F/ Ω cm^2	C_{dl}/ μF cm^{-2}s$^{\varphi 1-1}$
1300	2,893 ± 12	98.3 ± 0.4
1400	3,052 ± 73	106.0 ± 1.2
1450	3,618 ± 58	85.2 ± 0.6
1500	5,717 ± 139	84.3 ± 0.7
1550	4,100 ± 95	79.4 ± 0.9
1600	3,538 ± 45	75.9 ± 0.7
Electrooxidation of phenol at PtRu		
800	19,610 ± 361	109.0 ± 0.2
1000	51,429 ± 4,016	175.4 ± 1.2
1200	31,766 ± 2,152	115.2 ± 0.9
1400	5,526 ± 121	92.5 ± 1.1
1500	9,222 ± 173	68.3 ± 0.4
1600	7,931 ± 97	60.8 ± 0.3

The a.c. impedance behaviour of the phenol electrooxidation process at the PtRh and PtRu

electrodes, in contact with 0.1 M NaOH solution, is shown in Fig. 3 and Table 1. Thus, for the examined potential range 800-1600 mV, the impedance spectra exhibit single partial, somewhat depressed semicircles (contrast to the diffusion-controlled impedance behaviour recorded at polycrystalline Pt in 0.5 M sulphuric acid [3] for phenol concentration of 8×10^{-3} M). These partial semicircles (see examples recorded at 1500 mV in Fig. 3) correspond to the Faradaic phenol oxidation reaction (also, see equivalent circuit shown in Fig. 4). It should be noticed however that no time constant associated with the charge-transfer process accompanying electrosorption of reaction intermediates on the electrode surfaces could be identified in the recorded impedance spectra. The charge-transfer resistance, R_F parameter (see Table 1) corresponds to the oxidation process of phenol on the PtRh and the PtRu electrode surfaces. Hence, the R_F resistance reaches its minimum value of 2,893 Ω cm^2 (at 1300 mV) and 5,526 Ω cm^2 (at 1400 mV) for the PtRh and the PtRu electrodes, correspondingly.
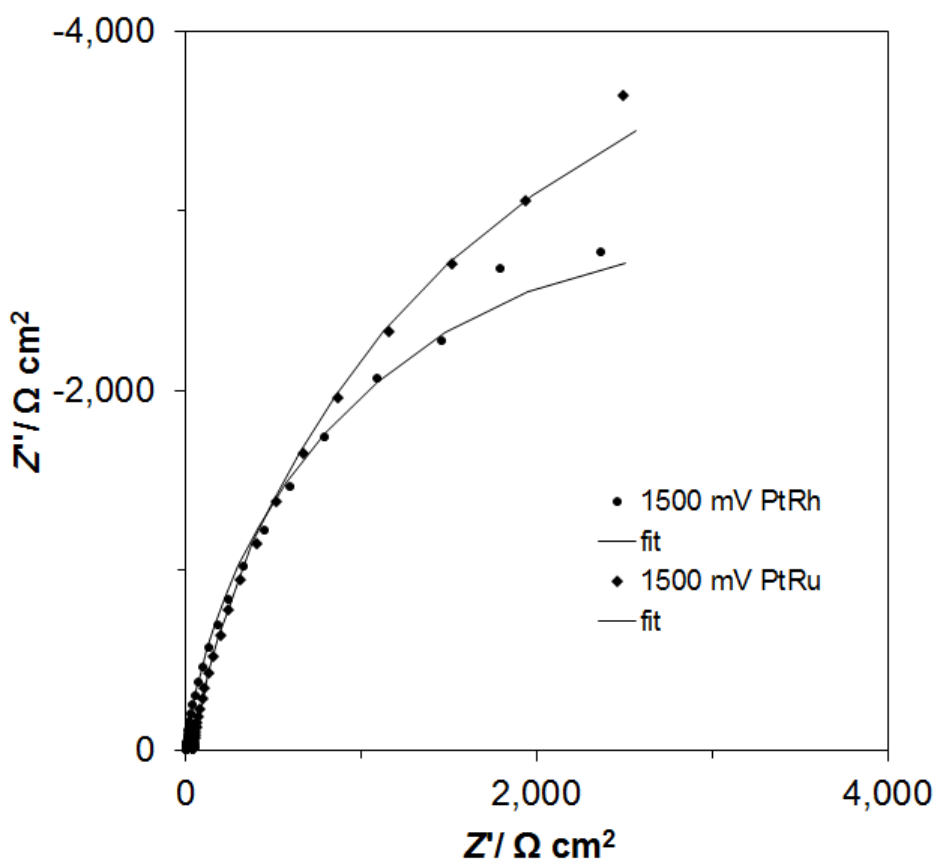

Figure 3. Complex-plane impedance plots for phenol electrooxidation on PtRh and PtRu electrode surfaces in contact with 0.1 M NaOH solution, recorded at room temperature for the potential of 1500 mV vs. RHE. The solid lines correspond to representation of the data according to equivalent circuit shown in Fig. 4.

Then, for the voltammetric peak potential value (*ca.* 1500 mV) the R_F parameter significantly increases to 5,717 and 9,222 Ω cm^2 for the PtRh and the PtRu electrodes, respectively. The latter effect is most likely related to increasing catalysts contamination by the reaction by-products, i.e. phenoxy

radicals. Then, subsequent reduction of the charge-transfer resistance parameter corresponds to an onset of the oxygen evolution reaction (see Table 1 and Fig. 2 again for details).

In addition, a capacitance dispersion effect (represented by distorted semicircles) can be observed in Nyquist impedance plots (see Fig. 3). Thus, the CPE-modified (constant phase element) equivalent circuit model (Fig. 4) was used to represent the electrochemical behaviour of the PhER in this work. The CPE behaviour is typically observed in case of inhomogeneous surfaces, displaying surface defects and porosity [15-17]. The double-layer capacitance, C_{dl} parameter (Table 1) oscillated between 75.9 and 106.0 $\mu F \ cm^{-2} \ s^{\varphi 1-1}$ (for PtRh), and 60.8 and 175.4 $\mu F \ cm^{-2} \ s^{\varphi 1-1}$ for the PtRu electrode. These C_{dl} values are dramatically higher than a commonly used C_{dl} value of 20 $\mu F \ cm^{-2}$ for smooth and homogeneous surfaces [18, 19]. The above implies considerable contribution from the surface electrosorption phenomena although the latter could not be identified from the performed impedance analysis. Also, a dimensionless φ_1 parameter, which determines the constant phase angle in the complex-plane plot ($0 \le \varphi_1 \le 1$) of the CPE circuit, varied between 0.85 and 0.95.
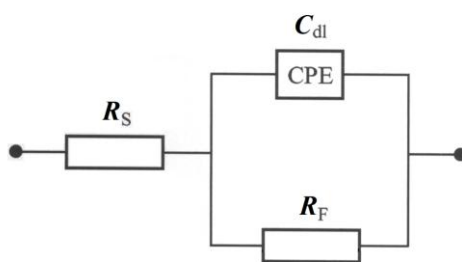
Figure 4. Equivalent circuit model for electrooxidation of phenol at PtRh and PtRu electrode surfaces, in the absence of adsorbed reaction intermediate(s). The circuit exhibits a Faradaic charge-transfer resistance, R_F in a parallel combination with the double-layer capacitance, C_{dl} (represented as the CPE), jointly in series with an uncompensated solution resistance, R_S.

4. CONCLUSIONS

The process of phenol electrooxidation in 0.1 M NaOH solution is strongly catalyst-dependent. Effective rates of an initial step of phenol oxidation are considerably faster on PtRh than those recorded on PtRu electrode surface. The above was proven both through the cyclic voltammetry, as well as the a.c. impedance spectroscopy analyses. Electrooxidation of phenol proceeds in the presence of surface-adsorbed reaction intermediates, which tend to progressively block the catalyst surface and inhibit the phenol oxidation process. However, an adsorption step was practically indiscernible within the recorded Nyquist impedance spectra. Finally, the recorded here minima of the charge-transfer resistance parameter for PhER on both the PtRh and the PtRu catalysts surfaces were radically higher than that recently derived [20] in this laboratory for a polycrystalline Pt electrode (2,005 $\Omega \ cm^2$) under

analogous experimental conditions, thus reflecting superior, electrocatalytic properties of the Pt material.

References

1. R.A. Torres, W. Torres, P. Peringer and C. Pulgarin, *Chemosphere*, 50 (2003) 97.
2. D. Rajkumar and K. Palanivelu, *J. Hazard. Mater.*, B113 (2004) 123.
3. C. Pirvu, A. Banu, O. Radovici and M. Marcu, *Rev. Roum. Chim.*, 53(11) (2008) 1007.
4. G. Lv, D. Wu and R. Fu, *J. Hazard. Mater.*, 165 (2009) 961.
5. X. Yang, J. Kirsch, J. Fergus and A. Simonian, *Electrochim. Acta*, 94 (2013) 259.
6. X. Li, Y. Cui, Y. Feng, Z. Xie and J. Gu, *Water Res.*, 39 (2005) 1972.
7. H. Ma, X. Zhang, Q. Ma and B. Wang, *J. Hazard. Mater.*, 165 (2009) 475.
8. M. Li, C. Feng, W. Hu, Z. Zhang and N. Sugiura, *J. Hazard. Mater.*, 162 (2009) 455.
9. C. Zhang, Y. Jiang, Y. Li, Z. Hu, L. Zhou and M. Zhou, *Chem. Eng. J.*, 228 (2013) 455.
10. S. Andreescu, D. Andreescu and O.A. Sadik, *Electrochem. Commun.*, 5 (2003) 681.
11. G. Arslan, B. Yazici and M. Erbil, *J. Hazard. Mater.*, B124 (2005) 37.
12. T.A. Enache and A.M.O. Brett, *J. Electroanal. Chem.*, 655 (2011) 9.
13. B. Pierozynski, *Int. J. Electrochem. Sci.*, 7 (2012) 3327.
14. J.R. Macdonald, *Impedance spectroscopy, emphasizing solid materials and systems*, New York: John Wiley & Sons (1987).
15. T. Pajkossy, *J. Electroanal. Chem.*, 364 (1994) 111.
16. B.E. Conway, *Impedance Spectroscopy. Theory, Experiment, and Applications*, Barsoukov, E. & Macdonald, J.R. (Eds.), Wiley-Interscience, John Wiley & Sons, Inc., Hoboken, N.J., 4.5.3.8 (2005) 494.
17. W.G. Pell, A. Zolfaghari and B.E. Conway, *J. Electroanal. Chem.*, 532 (2002) 13.
18. A. Lasia and A. Rami, *J. Applied Electrochem.*, 22 (1992) 376.
19. L. Chen and A. Lasia, *J. Electrochem. Soc.*, 138(11) (1991) 3321.
20. B. Pierożyński, G. Piotrowska and T. Mikołajczyk, *Pol. J. Chem. Tech.*, (submitted).